Journal of the Ceramic Society of Japan 109 [6] 493-499 (2001)

Paper

Nanocomposite PLZT Ceramic Materials in Comparison with Other Processing Technique for Photostrictive Application

光誘起歪み応用ナノコンポジット PLZT セラミック材料のプロセス技法への依存

Aydin DOGAN,* Patcharin POOSANAAS, Isaac Robin ABOTHU,**
Sridhar KOMARNENI and Kenji UCHINO

International Center for Actuators and Transducers, Materials Research Laboratory, The Pennsylvania State University, University Park, PA 16802 USA
**Ceramic Engineering Department, Anadolu University, Eskisehir, Turkiye*
***Institute of Materials Research and Engineering (IMRE), Singapore, 119260*

The performance of photostrictive materials can be enhanced by controlling the materials and microstructural characteristics through processing methods, ceramic composition and dopant type/content. In this paper the influence of ceramic processing methods on microstructure and photostrictive responses of Lanthanum modified Lead Zirconate Titanate (PLZT) ceramics have been investigated. Here we have investigated the recent technique of nanocomposite processing which showed good potential for the fabrication of photostrictive materials with enhanced properties. A significant enhancement of photovoltage and photocurrent which led to higher energy conversion ratio has been observed with decreasing grain size of PLZT ceramics with various processing techniques. [Received October 25, 2000; Accepted March 22, 2001]

Key-words : *PLZT, Nanocomposite, Sol-Gel, Photostriction, Photocurrent, Photovoltage*

1. Introduction

Photostrictive effect is the superposition of the photovoltaic and piezoelectric effects. Materials exhibiting the photostrictive effect have been the focus of attention for their potential usage as wireless photodriven actuators, relays, and microrobots. (Pb, La)(Zr, Ti)O_3 (PLZT) ceramics doped with WO_3 exhibit large photostriction under uniform illumination of near-ultraviolet light.[1)-3)] These materials are also promising candidates for use in photoacoustic devices (e.g., photophones) in optical communication systems.[3),4)]. The photostrictive properties of PLZT ceramics are influenced by material parameters (e.g., composition and stoichiometry, dopant type and concentration) and processing conditions (e.g., processing route and parameters).

It has been shown that the microstructure, especially the grain size of PLZT, has a strong influence on the photovoltaic effect. Conventionally, PLZT ceramics are synthesized by oxide mixing processes, where individual oxides are mixed in ball mills and reacted in the solid state.[2),3),5),6)]. The high temperature required for the large diffusion distances in the solid-state reaction of the metal oxides/carbonates, often result in low density PLZT products, with compositional and structural inhomogeneities. Non-conventional routes, such as sol-gel technique, have received wide attention due to the possibilities of overcoming these limitations for the PLZT processing.[7)-9)]

Sol-gel methods using alkoxides, evaporation of solution methods, a variety of precipitation methods, and hydrothermal techniques have been reported to yield pure, homogeneous and easily sinterable PLZT powder which offers distinct advantages such as lower processing temperature, better control over stoichiometry and higher chemical homogeneity. However, the excessive cost and special handling requirements for extremely moisture sensitive alkoxide precursors discourage the adoption of these techniques for routine ceramic synthesis. Recently, an innovative low temperature nanocomposite processing technique has been proposed, which offers an attractive alternative to these chemical synthesis routes to overcome large diffusion distances. This nanocomposite technique was developed by Roy et al. in the early 1980s.[10)] Nanocomposites are mixtures of two or more phases having different compositions or structures, where at least one of the phases is on a nanoscale (1-20 nm). At these sizes, materials begin to exhibit unique behavior that can be taken advantage of in terms of both processing methods and selection of the final application. With regard to electronic ceramics, nanosized powders may be used to enhance electronic properties by manipulation of characteristics such as grain size, density, purity and porosity. The high surface area of these powders correlates to a high degree of reactivity and a reduction of sintering temperature. Electroceramics prepared by a nanocomposite method have higher density than those processed through monophasic sol-gel route, and other common processing techniques, due to the lower differences between crystallization and densification temperatures.[11)-13)] Also, the impurities which are introduced into the system during intermediate calcinations and grinding steps of the conventional solid-state method can be eliminated in this method.

In order to utilize the photostrictive materials for commercial application their performance and efficiency need to be further improved. Increasing the performance of photostrictive materials will also open up numerous applications such as contactless actuators. A detailed and systematic evaluation (e.g., microstructure, photostrictive properties) of PLZT ceramics prepared through different routes (e.g., oxide mixing, chemical route, and nanocomposite technique) is highly desirable to assess the advantages and limitations of available ceramic processing techniques. The present research was aimed towards improving the performance of photostrictive materials by investigating the processing techniques of lanthanum-modified lead zirconate titanate (PLZT) ceramics for photostrictive property.

2. Experimental procedure

PLZT (3/52/48) ceramics with 3 at% La and a Zr/Ti ratio of 52/48 was selected due to its highest photovoltaic effect.[1)] PLZT ceramics were fabricated by four different

processing routes, namely, (i) conventional oxide mixing process, (ii) sol-gel technique, (iii) coprecipitation, and (iv) nanocomposite processing techniques. The details of the conventional oxide mixing and sol-gel techniques have been reported earlier.[7] In this study we mainly focused on nanocomposite preparation and comparison with other preparation techniques. The flow chart for sample preparation by nanocomposite technique is shown in Fig 1.

The density of the sintered samples was determined by the Archimedes method while microstructure and grain size of the samples were observed by scanning electron microscopy (SEM; ISI DS-130). In order to identify phases present in the powders, X-ray diffraction (Scintag Diffractometer) was carried out under Cu Kα radiation. Samples (10 mm in diameter and 1 mm in thickness) for dielectric measurement were polished, and then electroded with platinum (Pt) by sputtering. Dielectric properties of PLZT samples were measured with an impedance analyzer (HP-4274A). Samples for piezoelectric measurement were of the same dimension as for dielectric measurements, except they were poled in silicone oil at 120°C under a 2 kV/mm electric field for 10 min. Piezoelectric properties of all the samples were measured by using a Berlincourt d_{33} meter (Channel Products, Inc.) at 100 Hz.

Photovoltaic measurements were performed using a high-input-impedance electrometer (Keithley 617), while the photostriction was measured by a displacement sensor (LVDT; Millitron model 1301). Experimental set up to measure the photo induced strain, voltage and current is shown in Fig. 2. These measurements were done by radiating the light perpendicular to the polarization direction. The samples of $5\times5\times1$ mm^3 were cut and polished to size for these measurements. The 5×1 mm^2 surfaces were silver electroded. Poling was performed by applying 2 kV/mm electric field for 10 min in silicone oil at 120°C. A high-pressure mercury lamp (Ushio Electric, USH-500D) was used as a light source for the measurement. The white radiation was passed through an IR blocking filter (>700 nm) and an UV bandpass filter (between 248-390 nm) to obtain a beam with a maximum strength around 366 nm and an intensity of 3.25 mW/cm^2, before illuminating the samples (5×5 mm^2 polished surface). Light with this wavelength has been selected to yield the maximum photovoltaic properties.[14),15)] The photovoltage and photocurrent were determined from the current voltage relation by applying voltage between -100 and $+100$ V while illuminating the samples. The photovoltage and photocurrent were determined in an open circuit state from the intercept of the horizontal applied voltage axis while the photocurrent was obtained for the short circuit state from the intercept of the vertical current axis. Under exposure to UV radiation, a weak pryroelectric current was initially observed which reached a constant value after several seconds. Measurements were performed after the samples were thermally equilibrated with the radiation.

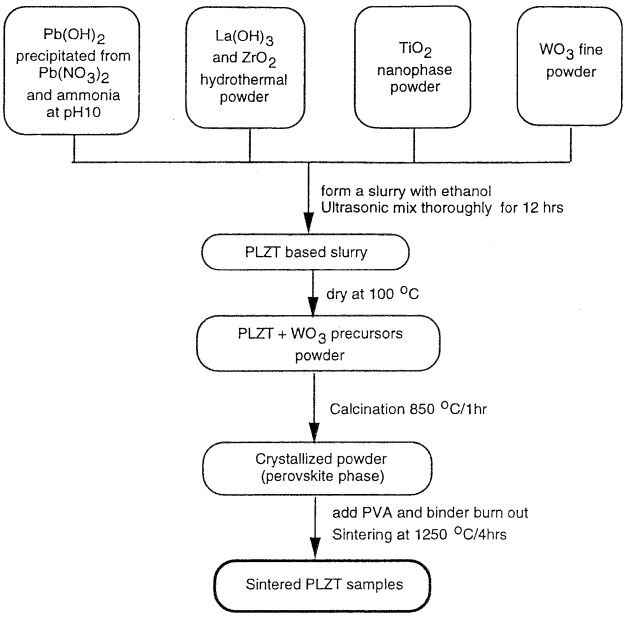

Fig. 1. Flow diagram of 0.5 at% WO_3 doped PLZT ceramics prepared by nanocomposite technique.

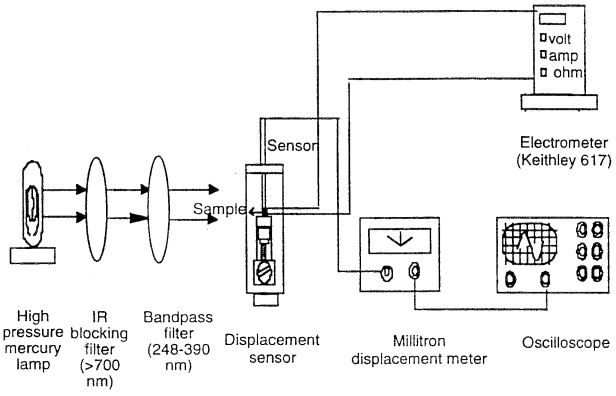

Fig. 2. Experimental set up for photovoltaic and photostrictive measurements.

3. Results and discussion

3.1 Characterization of PLZT Powder

Figure 3 shows the X-ray diffraction patterns of the oxide mix powders which were heat-treated at various temperatures. Crystallization of the perovskite phases during thermal treatment can be observed in samples thermally treated at 950°C for 10 h.

Corresponding patterns of slurry mixed nanocomposite powders, heat-treated for 1 h from 650 to 850°C are shown in Fig 4. The nanocomposite powder required a heat treatment at 850°C for 1 h to initiate crystallization of PLZT phase. The split of peaks at lower temperature was observed in this pattern due to a mixture of $LaTiO_3$, and PLZT. However, complete crystallization of the PLZT

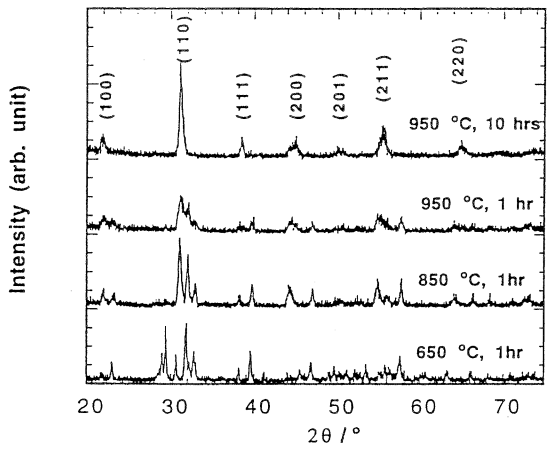

Fig. 3. XRD patterns of 0.5 at% WO_3 doped PLZT (3/52/48) oxide mixing powder with different heat treatment temperatures.

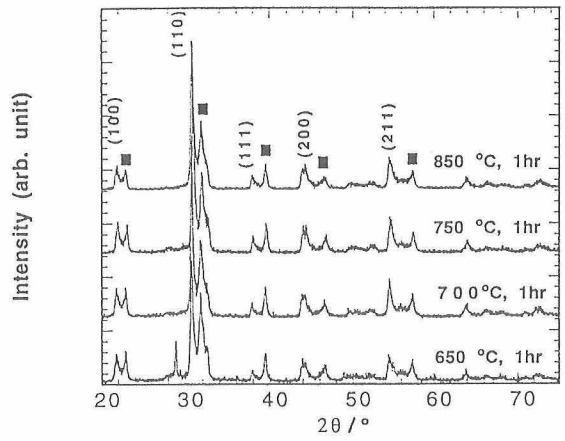

Fig. 4. XRD patterns of 0.5 at% WO_3 doped PLZT (3/52/48) nanocomposite powder with different heat treatment temperatures. "Filled boxes" represents Lanthanum Titanium Oxide peaks.

perovskite phase occurred after heat treatment at a higher temperature of 1250°C for 4 h. Similar observations have been made in the processing of fine powders of some other electroceramics. For example, powders of $BaTiO_3$ obtained at lower temperature need to be heated beyond 1150°C to form the tetragonal phase.[16),17)]

Fine sized, well-dispersed powders are desired as starting raw materials for processing of electroceramics. Agglomeration of fine powders is a major problem in the fine particles processed through chemical synthesis techniques, as it results in poor densification, microstructural inhomogeneities, and consequently, nonoptimal mechanical and electrical properties. SEM micrographs of calcined powders prepared by different techniques, oxide mixing process, sol-gel, and nanocomposite techniques are shown in Figs. 5 (a)-(c), respectively. It is evident from Fig. 5(a) that the oxide mixing process resulted in powders with the largest particle size (maximum size about 1 μm) and a broad particle size distribution. Although the sol-gel and nanocomposite techniques yielded similar fine spherical PLZT particles with average particle sizes in the range of 100–150 nm, they have different degrees of agglomeration. Sol-gel processed powders showed higher number of agglomerates compared to nanocomposite powders (Fig. 5(b)). The nanocomposite technique yielded fine PLZT powders with morphology similar to the sol-gel processed powder, but with significantly less agglomeration (Fig. 5(c)).

3.2 Characteristics of sintered PLZT ceramics

3.2.1 Densification characteristics

The densification behavior of powders is very important due to its strong bearing on the physical, mechanical and electrical properties of the final product. Figure 6 shows the relative sintered density of 0.5 at% WO_3 doped PLZT ceramic prepared by nanocomposite technique as a function of sintering temperature after 2 h of sintering in comparison with other processing methods.

In the oxide mix samples, the relative density initially increased with increase in sintering temperature and attained a maximum value of 98% at 1200°C. The sintered density remained constant even though the sintering temperature was further increased to 1300°C. In the sol-gel derived PLZT, a maximum density of 93% was observed at a sintering temperature of 1250°C for 2-h sintering time. The sintered density decreased as the sintering temperature was further increased. This may be attributed to lead loss due to the evaporation of PbO during sintering. A relative density

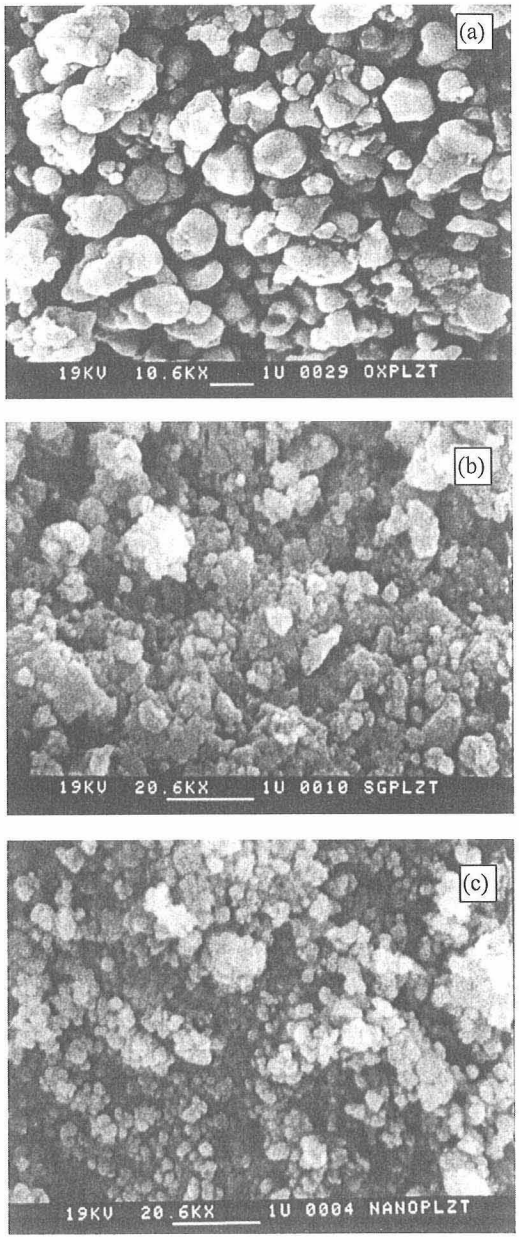

Fig. 5. SEM micrographs of 0.5 at% WO_3 doped PLZT calcined powder prepared frrom (a) the conventional oxide mixing process, (b) sol-gel technique, and (c) nanocomposite technique. (bar: 1 μm)

of 90% was obtained by the nanocomposite PLZT ceramics sintered at 1250°C for 2 h. Further increase on the sintering time increases densification and a relative density of more than 95% was attained by the nanocomposite PLZT ceramics sintered at 1250°C for 4-h sintering. Better densification in samples prepared from nanocomposite powders compared to sol-gel samples was achieved, (Fig. 8 and Table 1).

As is evident from Fig. 6, the sol-gel PLZT exhibited lower density as compared to the oxide mixed PLZT at all sintering temperatures. This lower density may be attributed to particle agglomeration in sol-gel derived materials (Fig. 5(b)). The high density in the oxide mixed PLZT samples is due to a broader particle size distribution obtained in this process (Fig. 5(a)), which yields a higher packing density.

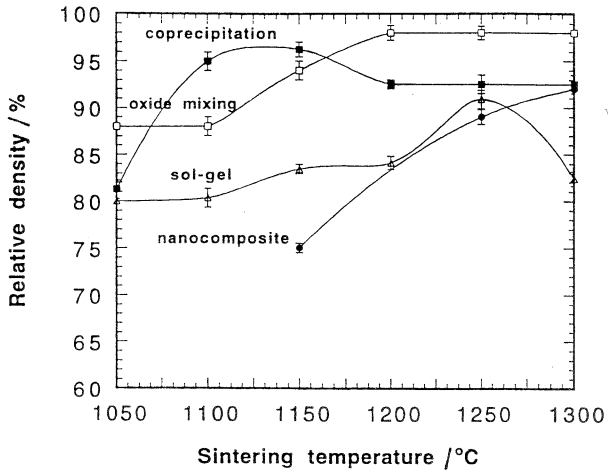

Fig. 6. Relative density of sintered 0.5 at% WO_3 doped PLZT (3/52/48) ceramics as a funciton of sintering temperature after 2-h sintering time.

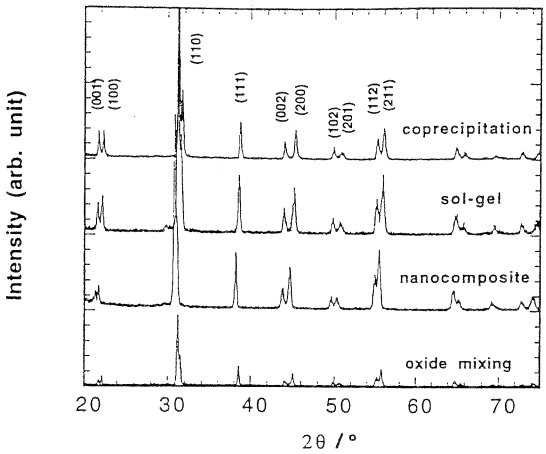

Fig. 7. XRD patterns of sintered 0.5 at% WO_3 doped PLZT (3/52/48) samples derived from different techniques.

3.2.2 Phase analysis

Figure 7 shows the XRD patterns for PLZT samples derived from nanocomposite technique in comparison with other techniques. The sintering conditions corresponding to the highest density were selected for each preparation technique. As is evident from this figure, all the samples form perovskite tetragonal phases. The XRD patterns are in good agreement with the JCPDS (Joint Committee on Powder Diffraction Standards) file number 29-776 for PLZT ceramics. The lattice parameters for these four techniques were calculated and shown in Table 1. It is clearly seen that PLZT derived from oxide mixing, sol-gel and coprecipitation, show similar c/a ratio. However nanocomposite PLZT exhibited the lowest c/a ratio (tetragonality) as compared to other techniques.

Table 1. Comparison of Ceramics Derived from Three Different Processing Techniques

Conditions/ Properties	Conventional oxide mixing	Nanocomposite technique	Sol-gel technique	Coprecipitation technique
Calcination	950 °C, 10h	850 °C, 1h	600 °C, 1h	550 °C, 1h
Sintering	1270 °C, 2h	1250 °C, 4h	1250 °C, 2h	1150 °C, 4h
Maximum relative density (%)	98%	95%	93%	99%
Average grain size (μm)	1.87±0.21	1.62±0.18	1.60±0.10	1.08±0.09
Lattice parameter (nm) a and c	0.40334 0.41147	0.40577 0.41308	0.40352 0.41146	0.40189 0.41046
Tetragonality (c/a ratio)	1.020	1.0180	1.020	1.021
Piezoelectric constant d_{33} (x 10^{-12} m/V)	320±4	315±5	315±4	310±8
Curie temperature (°C)	300	290	299	299
Maximum dielectric constant	15200	13500	12700	10000
Dielectric constant (at T_R)	1600±14	1250±16	1235±15	1220±16
Photovoltage, E_{ph},* (V/cm)	1500±31	1636±61	1650±38	2010±46
Photocurrent (nA/cm) *	1.7±0.14	2.46±0.32	2.48±0.21	2.5±0.25
Photoinduced strain * (x 10^{-5})	4.50±0.21	4.90±0.17	4.94±0.20	6.10±0.30
Calculated (d_{33} x E_{ph})	4.80	5.15	5.20	6.23

* For the illumination intensity 3.25 mW/cm^2

3.2.3 Microstructure analysis

Microstructures of WO_3 doped PLZT ceramics were examined by scanning electron microscopy (SEM), and the average grain sizes were determined by the intercept method. Figures 8(a)–(c) show the SEM micrographs of samples prepared by oxide mixing, sol–gel and nanocomposite techniques, respectively. The average grain sizes for oxide mixing, nanocomposite, coprecipitation, and sol–gel samples are listed in Table 1. The grain size was the smallest for the coprecipitated ceramics, whereas oxide-mixing process resulted in largest grain sizes. The powders prepared through the chemical routes are more reactive in nature and require a lower sintering temperature. This results in the lower average grain size of ceramics prepared by chemical synthesis as compared to powders obtained by solid-state reaction. Samples synthesized using the nanocomposite route yielded grain sizes similar to the sol–gel derived samples.

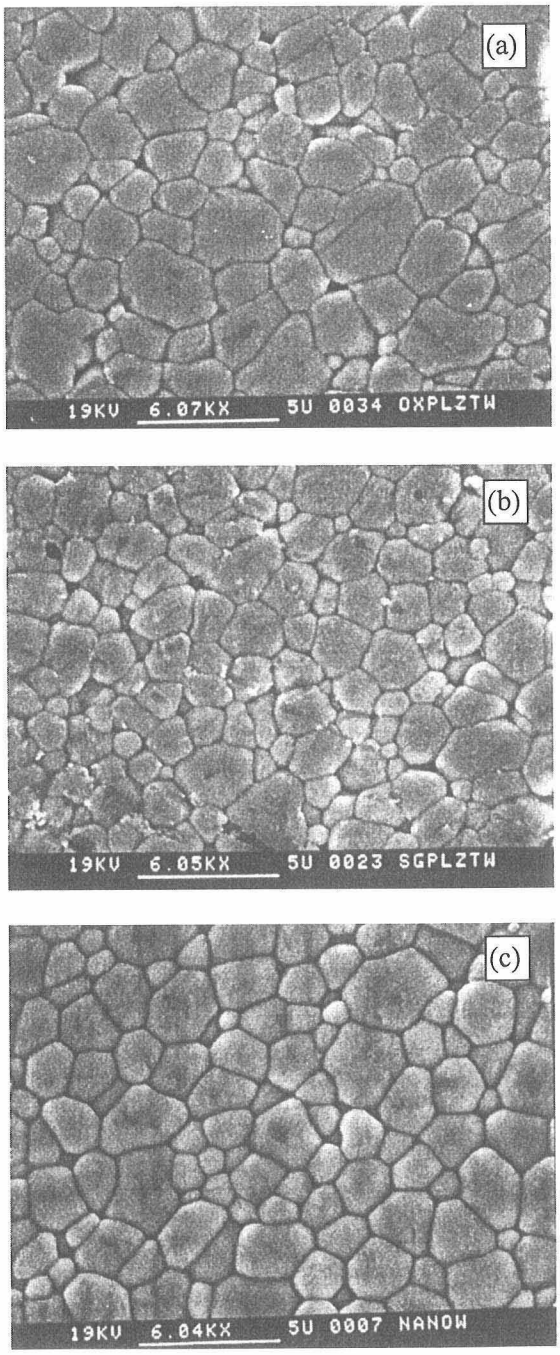

Fig. 8. SEM micrographs of 0.5 at% WO_3 doped PLZT ceramics prepared by (a) conventinal oxide mixing process, (b) sol–gel technique and (c) nanocomposite technique. (bar: 5 μm)

3.3 Dielectric and piezoelectric properties of PLZT ceramics

The variation of the dielectric permittivity as a function of temperature for the sintered WO_3 doped PLZT ceramics measured at 1 kHz is shown in Fig. 9. There are significant differences in the maximum dielectric constant peaks, which correspond to the Curie temperature (T_C), between the samples prepared by oxide mixing and copreciptation techniques. On the other hand, PLZT derived from nanocomposite technique had a lower T_C. This can be explained on the basis of the lower c/a ratio (tetragonality) observed in this technique (Table 1). Compositional fluctuation on the grain boundary may also cause changes on the dielectric constant. Grain size dependence of Maximum and room temperature dielectric constant of PLZT ceramics with various processing methods are shown in Fig. 10. As is well known, decreasing grain size decreases maximum and in general decreases room temperature dielectric constants to certain level. PLZT ceramics derived from nanocompo-

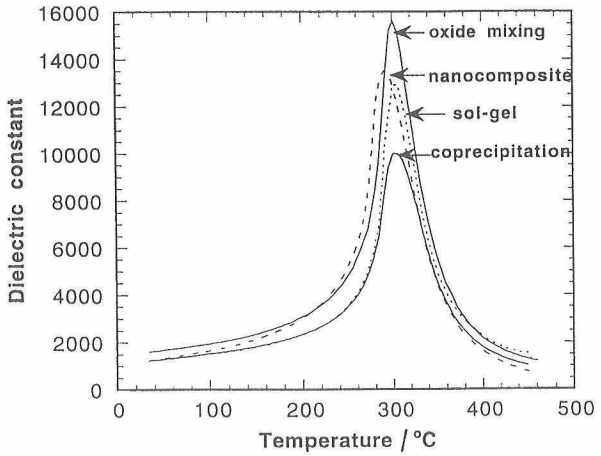

Fig. 9. Dielectric constant as a function of temperature at 1 kHz for 0.5 at% WO_3 doped PLZT samples fabricated from different techniques.

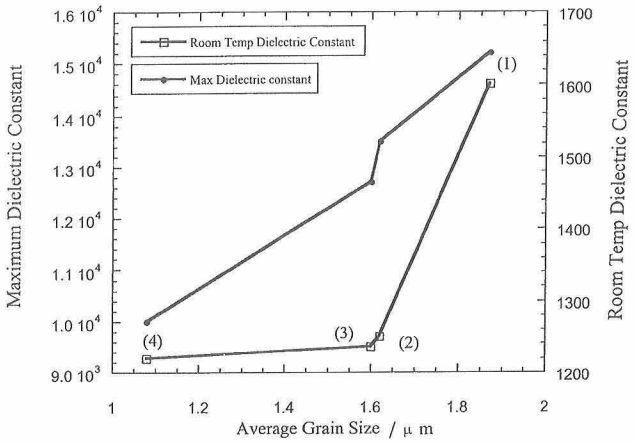

Fig. 10. Grain size dependence of dielectric constant of the PLZT ceramics prepared by different techniques.

site and sol-gel techniques exhibited lower dielectric constants as compared to that of the PLZT prepared by oxide route due to smaller grain size in the former. The reason of this behavior can be explained as follows: As the grain size decreases, the domain size and population and eventually the dielectric constant decrease. This phenomenon has been already observed for other piezoelectric ceramic materials. The piezoelectric constant d_{33} showed a similar tendency for the ceramics prepared by three different methods with the maximum for oxide mixing sample (Table 1).

3.4 Photovoltaic and photostrictive properties of PLZT ceramics

The physical properties of doped PLZT ceramics produced from three different processing methods are listed in Table 1 in comparison with nanocomposite technique. As shown in this table, depending on the processing technique, samples with the same composition can exhibit different photovoltaic and photostrictive properties. The photo-induced electric field reached more than 1 kV/cm and a photocurrent density on the order of nA/cm was achieved under the illumination intensity of 3.25 mW/cm^2 for 366 nm wavelength. Figure 11 shows the grain size dependence of photo-current and photo-voltage of PLZT ceramics prepared from the four different methods under the illumination intensity of 3.25 mW/cm^2. The grain size dependence of photo-current and photo-voltage were plotted by neglecting the effects which may come from various processing methods. It must be kept in mind that various preparation methods have merits and demerits. Eventually, grain size dependence should be studied on each processing method separately. Decreasing grain size enhanced the photovoltage and photocurrent. Decreasing the grain size from 1.87 to 1.08 μm increased both photo-current and photo-voltage roughly by about 35%.

Because PLZT is a photo driven transducer, appropriate comparison should be based on the energy conversion ratio of the transducer regarding the consumed energy and converted electrical energy.

$$\eta = \frac{\text{Converted Electrical Energy}}{\text{Input Light Energy}} \tag{1}$$

Only a certain portion of the illumination will transmit through the sample whereas some portion will be reflected from the illumination surface. The incident radiation is absorbed as it penetrates into the crystal lattice of a sample. The reflected amount of the light can be calculated from the Fresnel's Formula of reflection at optical region.

$$R = \left(\frac{n-1}{n+1}\right)^2 \tag{2}$$

The amount of light intensity reaching to a depth of x into the sample can be calculated from the following equation.[18]

$$I_{(x)} = TI_{(0)} \exp(-\alpha x) \tag{3}$$

Where the $I_{(x)}$ is the light intensity at the depth x and T is the transmittance at the sample surface. Using the equations above, the absorption coefficient of PLZT (3/52/48) doped with 0.5 at% WO_3 was found to be 0.0252 μm^{-1} at 366 nm. Reflected amount of the light is calculated as of 23% based on measured refractive indices of same composition material which is 2.89. The sample thickness was enough (1 mm) to absorb all the transmitted light. Hence, only 2.47 mW/cm^2 of the illuminated light intensity (3.25 mW/cm^2) will be used by the sample and the rest will be reflected.

Converted and stored electrical energy can be calculated by the following equation:

$$E_{\text{Maxout}} = \frac{1}{2} J_{\text{ph}} E_{\text{ph}} \tag{4}$$

Hence the equation for the efficiency of the transducer will be;

$$\eta = \frac{\left(\frac{J_{\text{ph}} E_{\text{ph}}}{2}\right)}{(I_{\text{in}})} \tag{5}$$

Calculated efficiency of the transducers based on the measurements for PLZT ceramics made of various ceramic processing methods and grain size is shown in Fig. 12. As it is seen in the figure the energy conversion efficiency increased with decreasing grain size. The conventional oxide mixing method with the larger grain size showed the smallest efficiency. Sample made by the coprecipitation technique with the lowest grain size showed the highest efficiency. Samples fabricated with the sol-gel and nanocomposite techniques exhibit almost similar energy efficiencies.

Nanocomposite PLZT samples exhibited photovoltaic and photostrictive properties comparable to those observed in

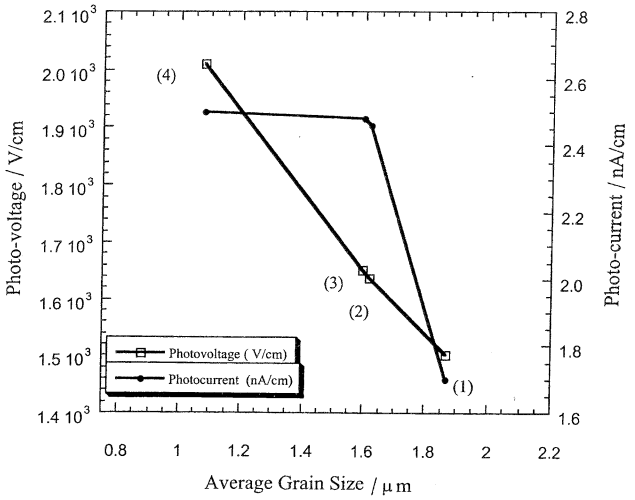

Fig. 11. Grain size dependence of photovoltage and photocurrent of the PLZT ceramics prepared by different techniques.

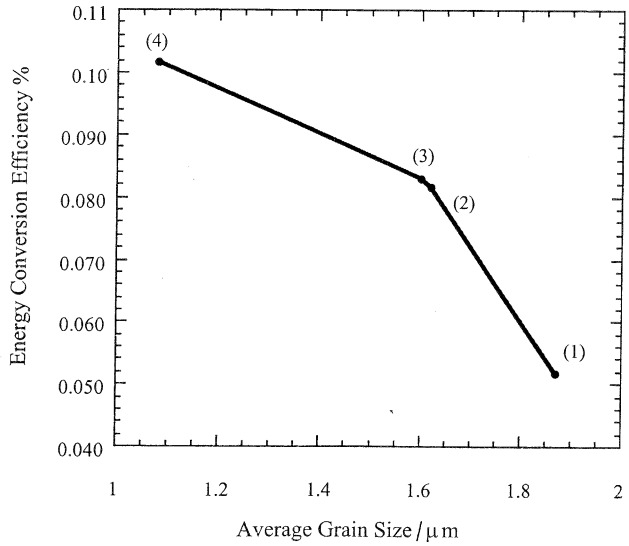

Fig. 12. Grain size dependence of energy conversion efficiency of the PLZT ceramics prepared by different techniques.

the sol-gel PLZT. These properties are larger than those observed in PLZT derived from oxide mixing reactions. Table 1 also lists the calculated product values of piezoelectric constant d_{33}, and photo-induced electric field E_{ph}, which are in good agreement with the experimental data.

4. Conclusion

The processing method used to synthesize a ceramic sample determines the homogeneity, stoichiometry, and grain size of the product, which in turn strongly affect its photovoltaic and photostrictive properties. In general, high levels of impurities and inhomogeneities are expected in ceramics prepared by solid state reaction when compared to those observed in samples prepared by chemical synthesis routes. Ceramics prepared by nanocomposite and sol-gel techniques exhibit high purities and desirable properties such as higher degrees of homogeneity, uniform distribution of dopant and closer control of stoichiometry. The atomic level interaction and mixing along with finer particle size requires a lower sintering temperature and produces ceramics with smaller grain sizes in chemical synthesis technique.

The strong dependence of photovoltage on the grain size led to superior photovoltaic and photostrictive properties in the samples prepared by nanocomposite and sol-gel techniques as compared to the oxide mixing process. However, the lower relative density of ceramics prepared by sol-gel route appears to be a major limitation for this technique. The relatively small difference between crystallization and densification temperatures in the nanocomposite technique resulted in higher density ceramics. This recent technique appears to have good potential for fabrication of photostrictive PLZT ceramics.

The energy conversion efficiency for the fabricated PLZT photovoltaic materials is around 0.1%. Further enhancement can be developing by establishing a technology for improving the density while keeping the grain size as small as possible.

References

1) Uchino, K. and Aizawa, M., *Jpn. J. Appl. Phys.*, **24**, 139–41 (1985).
2) Tanimura, M. and Uchino, K., *Sensors and Materials*, **1**, 47–56 (1988).
3) Chu, S. Y. and Uchino, K., *J. Adv. Performance Mater.*, **1**, 129–43 (1994).
4) Uchino, K., *Mechanical Automation*, **21**, 34 (1989).
5) Sada, T., Inoue, M. and Uchino, K., *J. Ceram. Soc. Japan (Yogyo-Kyokai-Shi)*, **95**, 545–50 (1987) [in Japanese].
6) Nonaka, K., Akiyama, M., Takase, A., Baba, T., Yamamoto, K. and Ito, H., *J. Mater. Sci. Lett.*, **15**, 2096 (1996).
7) Poosanaas, P., Dogan, A., Prasadarao, A. V., Komarneni, S. and Uchino, K., *J. Electroceramics*, **1**, 105–11 (1997).
8) Poosanaas, P., Dogan, A., Prasadarao, A. V., Komarneni, S. and Uchino, K., *J. Adv. Performance Mater.*, **6**, 57–69 (1999).
9) Choy, J. H., Han, Y. S. and Kim, J. T., *J. Mater. Chem.*, **5**, 65 (1995).
10) Roy, R., Komarneni, S. and Roy, D. M., *Mater. Res. Soc. Symp. Proc.*, **32**, 347–59 (1984).
11) Prasadarao, A. V., Abothu, I. R. and Komarneni, S., "Ceramic Transactions," Vol. 70, Ed. by Hiremath, B., Gupta, T. and Nair, K. M., Am. Ceram. Soc. (1997) pp. 253–60.
12) Prasadarao, A. V., Abothu, I. R. and Komarneni, S., *Ferroelectrics Lett.*, **21**, 141–50 (1996).
13) Brody, P. S., *J. Solid State Chem.*, **12**, 193 (1975).
14) Nonaka, K., Akiyama, M., Takase, A., Baba, T., Yamamoto, K. and Ito, H., *Jpn. J. Appl. Phys.*, **34**, 5380 (1995).
15) Naka, S., Nakakita, F., Suwa, F. and Inagaki, M., *Bull. Chem. Jpn.*, **47**, 1168 (1973).
16) Vivekanandan, R., Philip, S. and Kutty, T. R. N., *Mater. Res. Bull.*, **22**, 99 (1986).
17) Vivekanandan, R. and Kutty, T. R. N., *Powder Technol.*, **57**, 181 (1989).
18) Poosanaas, P., Dogan, A., Thakoor, S. and Uchino, K., *J. Appl. Phys.*, **84**, 1508–12 (1998).